

# Steady State Analysis of Water Transport through Sulfonated Polyether Ether Ketone (SPEEK) Membrane for Fuel Cell Application

RABIRANJAN MURMU<sup>1,2\*</sup> AND HAREKRUSHNA SUTAR<sup>1</sup>

<sup>1</sup>Department of Chemical Engineering, Indira Gandhi Institute of Technology, Sarang, 759146, Odisha, India.

<sup>2</sup>Department of Chemical Engineering, Indian Institute of Technology Madras, 600036, India.

## ABSTRACT

*Sulfonated Polyether Ether Ketone (SPEEK) membrane is considered as a potential alternative membrane for fuel cell because of its cost effectiveness and easily prepared. SPEEK membranes were prepared by solution casting method with film thickness of 80, 127 and 150  $\mu\text{m}$ . Samples are analyzed by Fourier Transform Infrared (FTIR) Spectrometer. Water uptake study states that diffusivity of water increased with increase in Degree of Sulfonation (DS) of the membrane. Experimental moisture uptake data was fitted to a dual stage model. Proton conductivity of the membrane was measured by two probe method using impedance analyzer. Proton conductivity of the sample is improved with improving DS of membrane. Proton conductivity of membrane gave promising results in the range of  $10^{-2}$  to  $10^{-1}$  S/cm. Membrane water content has the greatest effect towards proton conductivity. The permeation of water through membrane was measured by in house permeation cell at a temperature range of 40-90°C and feed side water activity between 0.2 and 1. Water permeation from liquid feed increased with increase in membrane temperature and inversely proportional with membrane thickness. Water transported across the membrane in a permeation cell was considered as a one dimensional diffusion model. Water permeation data was compared with conventional Nafion permeation results. Water permeability data shows linear improvement with membrane water content and temperature.*

**KEYWORDS:** *Sulfonated Polyether Ether Ketone, Degree of sulfonation, Water activity, Diffusivity, Interfacial mass transport, Permeation Coefficient.*

## 1. INTRODUCTION

Due to the increase of consumption of petroleum based energy resource and depletion of fossil fuels, fuel cell technology received much more attention in recent years because of their high efficiencies and low toxic emissions. Fuel cell is a device that converts the chemical energy from a fuel into electricity through an electrochemical reaction using fuels such as hydrogen to electrical energy<sup>[1]</sup>. Fuel cell is classified based on the type of electrolyte used. Polymer electrolyte membrane (PEM) fuel cells are considered as a potential encouraging device because of their high efficiency and low operation temperature. In PEM fuel cell, the presence of water in the membrane affects fuel cell performance. Presence of water in the membrane enhanced proton transport, which is a very important framework of fuel cell<sup>[2-3]</sup>. Due to electrochemical reaction; water was produced at the cathode and must be absorbed and transported uniformly across the membrane. Knowledge of the kinetics of water sorption and transport in polymer electrolyte membranes is essential to optimize the design and operation of fuel cells.

At present Nafion membrane is considered as one of the most effective membrane for fuel cell. It is made up of perfluorosulfonated random copolymer with a tetrafluoroethylene backbone and perfluoroalkyl ether side chains terminated by sulfonic acid groups. Nafion membrane consists of phase separated hydrophilic domains of sulfonic acid groups and water absorbing hydrophobic domain of tetrafluoroethylene (TFE) and perfluoroalkyl ether (PFA). Water and protons are transported through the hydrophilic domains of Nafion

matrix. When water is absorbed by Nafion, hydrophilic domains swell and reorient its structure, which changes effective mass diffusion coefficient. Water transport through Nafion has been extensively investigated for three decades by several investigators adopting different methods. Most investigators wrongly assumed that the rate of water transport was controlled by Fickian diffusion<sup>[4-8]</sup>. In PEM fuel cell; proton conducting membrane is an important component to attain high power densities<sup>[9-11]</sup>. The requirements of fuel cell membranes are high proton conductivity, low reactant permeability, good mechanical and thermal stability, and low cost. Membrane materials being investigated for PEM fuel cell are generally classified as fluorinated polymers, partially fluorinated polymers, nonfluorinated or hydrocarbon polymers, and acid–base blends<sup>[12]</sup>. Nafion, a perfluorinated sulfonate dionomer, shows high proton conductivity, good mechanical properties, and thermal stability<sup>[10-11]</sup>. However, it shows some limitations like its poor barrier properties, dimensional stability, and poor performance at temperatures higher than 80°C<sup>[10-14]</sup>. Because of its relatively high cost, poor methanol crossover, low proton conductivity at high operating temperatures, and poor mechanical properties under swollen conditions, development of alternative polymer electrolyte membrane materials to Nafion is necessary<sup>[15]</sup>. Sulfonated poly (ether ether ketone) (SPEEK) is widely considered as a potential alternative because of its low methanol permeability, good thermal stability, and good proton conductivity. SPEEK membranes have been studied for their proton conductivity, at varying temperatures<sup>[15-17]</sup> and humidities<sup>[18]</sup>. Proton conductivity is strongly influenced by water uptake. In addition to the DS, the solvents

used for casting the membranes and the membrane preconditioning were found to affect properties such as the proton conductivity and the water uptake of SPEEK and the membrane electrode assembly performance due to variations in the microstructure [19]. The uptake and transport of water in the membranes of PEM fuel cells is essential to their operation [20-25], affecting both steady state and dynamic response. Membrane hydration is required for high proton conductivity. Water enters the membrane from either from humidified feeds or from product water generated at the cathode and diffuses through the membrane from high concentration to low. Since Nafion has long been the most common membrane material used in PEM fuel cells, numerous investigators have studied water uptake and water transport in Nafion [20, 23, 25, and 26].

Water management problem was the biggest issue for PEM fuel cell at low temperature operation. To overcome water management issue, lot of studies was carried out at more than 80°C for Nafion membrane. Results suggested by Majsztrik et al. state that at steady state water transport across Nafion membranes is independent of membrane thickness when liquid water was present at one interface, but the transport scales inversely with membrane thickness when both interfaces were exposed to water vapor. These results suggested the rate-limiting step for water transport was interfacial transport at the vapor/membrane interface when liquid water was present at one interface, but the rate limiting step was diffusion across the membrane when vapor was present at both interfaces. It was also found that the effective water diffusion

coefficient decreased with decreasing water activity, causing diffusion to become rate limiting at low water activity.

Now a day SPEEK membrane is considered as a potential alternative of Nafion membrane. Biggest drawback of a PEM fuel cell is the low performance at low temperature because of its poor water management ability. To rule out water management issue, fuel cell should be operated at high temperature condition. So this paper focuses steady state water permeation at high temperature. To understand the effect of water on fuel cell at high temperature, steady state water permeation was studied. Permeation experiments closely approximate the transport of water in to and through the membrane occurring in an operating fuel cell; mass transport at the membrane interfaces as well as diffusion through the membrane are present during steady state permeation. Experiments were designed to measure water permeation through SPEEK from vapor feeds of different activity, as well as from liquid water. Permeation was measured as a function of water activity and temperature.

## 2. EXPERIMENTAL

### 2.1. Materials

Bulk quantity of Victrex peek powder was purchased from sigma Aldrich, UK. Concentrated Sulfuric acid (98%), N-methyl pyrrolidene as a solvent, Caustic soda and Hydrochloric acid were purchased from local chemical suppliers at Talcher. Stainless steel electrode, rotameter, voltmeter, variable resistor and on/off valve used for permeation set up development was purchased from Sairaj electronic, Bhubaneswar. PTFE pipe, water heater was purchased from Talcher, Odisha.

### 2.2. Preparation of the membrane

Polyether ether ketone (PEEK) powder was dried in an oven for 8 hour at 65°C to remove the moisture content.

SPEEK membrane was prepared by solution casting method. Required amount (7.5 gm) of PEEK powder was dissolved to a 150 ml of concentrated sulfuric acid in a beaker at 45°C and vigorously stirred using magnetic stirrer for 2 hour. The entire reaction process was carried out in a fume hood. Later the reaction time was varied for preparing different DS of membrane. After reaction, product mixture was precipitated in ice cold water by using burette. Polymer obtained by this process was washed with distilled water several times to make it neutral (pH 6). Then the polymer beads obtained by precipitation process were kept in an open atmosphere for 18 hour. After that the beads were dried in oven at 60°C for 16 hour followed by 18 hour at 80°C to remove the residual moisture content. SPEEK granules obtained by this process were dissolved in an N-methyl-2-pyrrolidone solution for 18 hour at 60°C. Then the product mixture was cast in to a flat glass Petridis to make a sheet of thin film. The cast membranes were dried at 60°C for 12 hour followed by 80°C for 24 hour in a hot air oven to remove the volatile solvents. The resultant membranes were peeled off from the Petridis by using little amount of water on the side of Petridis. Finally the membranes were prepared and tested.

### 2.3. Ion Exchange Capacity (IEC) and DS

Ion Exchange Capacity of the membranes was determined by the titration method. Membrane was cut in small size and immersed in 0.1M HCL solution for 24 hour. Then the membrane was washed with distilled water till there was no free proton on its surface. Then the sample was immersed in 0.1M NaCl solution for 2 days to exchange protons with sodium ions. Then the exchanged protons within the solutions were titrated with a 0.01M NaOH solution with Phenolphthalein as an indicator. When the solution turned pink; titration was stopped. The volume consumed by the titration method was reported for calculating IEC and DS of membrane.

The IEC value was calculated by using this formula

$$IEC = \frac{M_{E,NaOH}}{W_d} \quad (1)$$

$M_{E,NaOH}$  is the mole equivalent of NaOH and  $W_d$  is the weight of dry membrane. The DS % was calculated from IEC using the following relation

$$DS = \frac{M_p \times IEC}{1 - (IEC \times M_f)} \times 100 \quad (2)$$

Where  $M_p$  is the molecular weight of the polymer repeat unit; without the functional group, and  $M_f$  is the molecular weight of the functional group with the counter ion ( $ASO_3Na$ ). By measuring the amount of  $H_2SO_4$  consumed in the titration, the molar quantity of the sulfonic acid groups ( $SO_3H$ ) contained in the SPEEK-H sample is determined and finally DS was estimated using eq-2. Variation of IEC and DS of SPEEK sample with reaction time was shown in figure 1. From the experimental results, it was found that IEC and DS of SPEEK sample increases linearly with reaction time. Improvement of DS from 65% to 92% achieved by varying the reaction time from 160 minute to 250 minute.

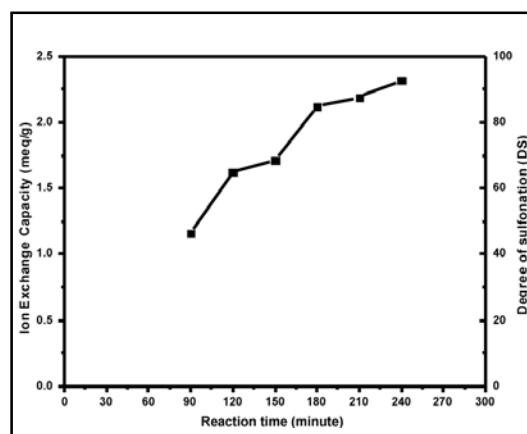


Fig. 1. Variation of IEC and DS with respect to reaction time.

### 2.4. Proton Conductivity

Proton conductivity of the membranes was measured by two probe method. An impedance analyzer with an electrochemical interface (GILL ACM Instrument, UK) was used in the frequency range of 1-300 kHz and voltage amplitude of 60 mV at 26°C.

The proton conductivity was calculated as follows:

$$\sigma = \frac{L}{RA} \quad (3)$$

Where  $\sigma$  is the proton conductivity in S/cm; L is the distance between the two electrodes used to measure the potential (L=1 cm); R is the membrane resistance derived from the low intersect of the high frequency semicircle on a complex impedance plane with the Re (z) axis; and A (width × thickness) is the surface area required for a proton to penetrate the membrane [27]. Proton conductivity data of SPEEK sample at different water content is shown in figure 2. Proton conductivity data were varied with membrane water content. Proton conductivity data were observed in the range of  $10^{-2}$  to  $10^{-1}$  S/cm. Maximum proton conductivity was  $1.43 \times 10^{-1}$  S/cm for DS (0.78) at 92% water content. Proton conductivity increased linearly with membrane water content up to a particular extent then drastically decreases. For high DS, membrane gave better proton conductivity due to the presence of more sulfonate group that absorbed more water. By absorbing more water, hydrophilic domain of SPEEK matrix expanded, that enhances better proton transport. When the membrane water exceeds from desired hydration level, proton transport decreased due to the formation of cluster that block flow channel of hydrophilic domain. For better proton conductivity, desired water

content should be maintained on the membrane. Presence of sulfonate group on SPEEK matrix influenced proton conductivity. Sulfonate group act as a carrier of proton across membrane. At fixed water content, membrane with DS (0.78) gave more proton conductivity than DS (0.56). It was concluded that membrane with high DS resulted in better proton conductivity.

### 2.5. Water uptake and diffusivity:

Water uptake capacity of the membrane was performed by weighing method. SPEEK membrane was cut to spherical shape (Surface area  $11.342 \text{ cm}^2$ ) and dried at  $60^\circ\text{C}$  for 15 minutes in a hot air oven before performing test. Dry weight of the sample was measured using a digital balance. Then the dry sample was immersed using a distilled water for 30 hours till equilibrium value achieved. At a particular interval of time wet membrane was taken out and ensured there was no water on the membrane surface by using tissue paper. Then immediately weight of the membrane was measured by digital balance. Experiment was stopped when steady weight of the membrane is achieved. The water uptake (WU) can be calculated by using following equation

$$WU(\%) = \frac{W_{\text{wet}} - W_{\text{dry}}}{W_{\text{wet}}} \quad (4)$$

Here  $W_{\text{dry}}$  and  $W_{\text{wet}}$  are the weight of dry and wet (equilibrium condition or hydrated) membrane respectively. Water uptakes of membrane were performed at various temperatures. Most of the researchers blindly assumed that the behavior of water uptake was controlled by Fickian diffusion. But the model proposed by Takamatsu et al. [28] and Morris and Sun [29] is most commonly used for analysis. Model equation proposed for Fickian diffusion is

$$\frac{M_t}{M_\infty} = \exp(-kt) \quad (5)$$

From equation-5, the slope of  $\ln \frac{M_t}{M_\infty}$  versus time gives an effective rate constant “k” for diffusion.

$$D = kL^2 \quad (6)$$

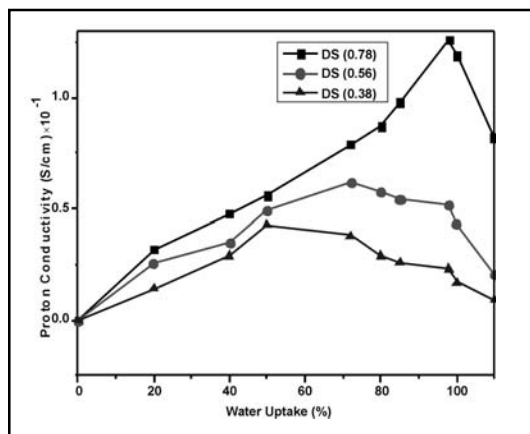


Fig. 2. Variation of Proton Conductivity with water content of different membrane.

Here  $L$  is the thickness of membrane,  $D$  is the diffusivity of water and  $k$  is the effective rate constant for diffusion. The theoretical model has good agreement with experimental data at initial stage of diffusion. But fit is not good at the entire diffusion process. During water uptake, two type of behavior was observed. At the initial stage of water uptake, water diffused with constant diffusivity and was controlled by Fickian behavior. But when more water was absorbed, water molecules bonded with polymer chain and diffusion rate reduces and relaxation rate increased. In this case, water uptake by diffusion was limited and diffusion

was governed by relaxation rate. A non Fickian behavior was observed at the later stage of diffusion. Both phenomena happened continuously during diffusion process. Both phenomena can be well explained by a dual stage model proposed by Mark D. Placette et al. [30]. For diffusion analysis, they considered a standard dimension of slab with constant diffusivity at a particular duration of time. Dual stage model give appropriate fit of experimental data. Dual stage model equation for absorption is reported in equation 7.

Here  $M_t$  is the sum of the moisture gain at the both stage of diffusion at time  $t$ ,  $M_{\infty, I}$  and  $M_{\infty, II}$  is the total moisture

$$M_t = M_{\infty, I} \left[ 1 - \frac{8}{\pi^2} \sum_{n=0}^{\infty} \frac{-1^n}{(2n+1)^2} \exp \left[ \frac{-(2n+1)^2 \pi^2 D_I t}{4L^2} \right] \right] + M_{\infty, II} \left[ 1 - \frac{8}{\pi^2} \sum_{n=0}^{\infty} \frac{-1^n}{(2n+1)^2} \exp \left[ \frac{-(2n+1)^2 \pi^2 D_{II} t}{4L^2} \right] \right] \quad (7)$$

gain at the initial and later stage of diffusion,  $L$  is the thickness of membrane,  $D_I$  and  $D_{II}$  are the initial and final stage of water diffusivity on polymer membrane.

### 3. Permeation measurement

#### 3.1. Permeation instrument

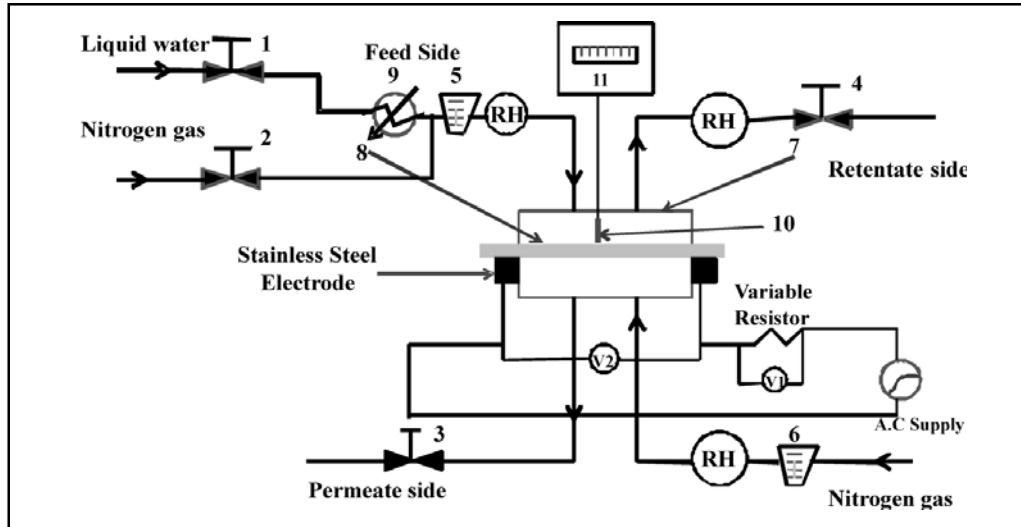
Water permeation through SPEEK membrane was measured in a recently modified permeation cell. In permeation cell, membrane was squeezed between two semicircular metal plates. Both Plates were bolted together with a membrane to separate two flow channels. Each halves of the metal plate were designed in such a way that it creates flow channel through which vapor or liquid could flow. Maximum operating temperature of the cell was in the range of 120-150°C. Inlet and outlet of the cell was connected by 0.25 inch PTFE pipe.

Water activity was introduced to the feed flow channel by flowing humidified Nitrogen.  $N_2$  gas is fed through the feed and sweep sections. For maintaining the water activity on feed channel additional water heater was used. Figure-3 was a schematic representation of the permeation cell along with all connecting pattern. The water activity of the  $N_2$  streams exiting both sides of the cell were separately measured using commercially available relative humidity sensors (HIH6130) installed in custom-built housings. The operating range of the humidity sensors was -25 to 110 °C and 10-90% RH. For liquid feed, a peristaltic pump provided for a constant

flow of liquid water. Humidified  $N_2$  feed was supplied on the cell by mixing dry  $N_2$  and humidified water streams. Humidified water was produced by heating liquid water on a 3/4th filled water bath by using water heater. Water activities on the feed side are maintained by controlling flow rate of  $N_2$  and humidified water. Water activity was obtained in the range of 0.1 to 0.9. The total flow rate of humidified feed stream has the range of 1 and 4 L/min, which ensured that the difference of water activity on the both sides of flow channel.  $N_2$  flow on the dry side of the cell was accurately maintained by mass flow controllers. For measuring membrane temperature, a temperature sensor was attached on the membrane surface. Heating of the membrane was done by alternating power supply with monitoring voltage and adjustable resistor. Constant voltage was supplied across the membrane to maintain the steady state temperature.

#### 3.2. Permeation Measurements Procedure:

Permeation of water from liquid water and vapor feed was measured by permeation cell shown in figure 1. A specific dimension of membrane was kept in the cell and liquid water or humidified stream was introduced on the feed side. Water was transferred from feed side to permeate side based on the activity difference between the two sides of cell. Experimental data was measured when steady state value was achieved. Temperature of the membrane was measured by a micro thermal sensor attached to its surface with digital input.



1,2,3,4—Valve,5,6-Rotameter,7-Permeation cell, 8-Membrane,9-Water heater, 10-Temperature sensor,11-Temperature Indicator, RH-Relative Humidity meter, V1,V2-Voltmeter

Fig. 3. Schematic representation of permeation cell set up

Uniform heating of the membrane was done by merged electrode with controlled supply voltage. To regulate supply voltage variable resistor with capacity  $3\Omega$  was used. Based on the knowledge of membrane temperature,  $T$ , relative humidity,  $RH$ , the dry  $N_2$  flow rate,  $Q$ , the water flux was calculated by following equation.

$$FLUX = \frac{Q \rho_g}{A_{mem} M_g} \frac{M_v \frac{RH}{100} p_{sat}}{(p_{tot} - \frac{RH}{100} p_{sat})} \quad (8)$$

$Q$  is the volume flow rate of dry  $N_2$  at the dry side with density  $\rho_g$ ,  $M_v$  is the molecular weight of water,  $M_g$  is the molecular weight of  $N_2$ ,  $p_{tot}$  is the total pressure of the water vapor/gas mixture (assumed to be 1 bar),  $p_{sat}$  is the saturation vapor pressure of liquid water at the temperature at which the relative humidity was measured, and  $A_{mem}$  is the area of the membrane.

Water transported through the membrane can be considered as a one dimensional diffusion model. The water flux through the membrane is strongly dependent on the water activity at feed and permeates side. Water transported through membrane by means of diffusion.

From the diffusion model, water flux is directly proportional to activity difference across the film. On feed side, mass transport depends on water activity between membrane surface and bulk side. So the general expression for water transport in feed side is given by

$$Flux = k_f (a_f - a_{mf}) \quad (9)$$

Here  $a_f$  and  $a_{mf}$  are the activity of water on bulk feed side and membrane surface. Similar expression can be used on dry side of permeation cell. Water transport on the dry side is given by

$$Flux = k_d (a_{md} - a_d) \quad (10)$$

Where  $k_f$  and  $k_d$  is the mass transfer coefficient on feed and permeate side respectively. Water flux through the membrane is by means diffusion. Now applying Fick's law across the membrane, we get

$$Flux = \frac{D}{L} (a_{mf} - a_{md}) \quad (11)$$

Here  $D$  is the diffusion coefficient and  $L$  is the thickness of membrane. So in a one dimensional permeation cell, water is transported by means of diffusion and interfacial mass transport. Resistances of water transport through membrane arise due to interfacial mass transport and diffusion. Overall mass transfer coefficient can be written as

$$K_o = \frac{\frac{D}{L} k_f k_d}{\frac{D}{L} k_d + \frac{D}{L} k_f + k_f k_d} \quad (12)$$

From equation (12), it is observed that if rate of mass transport is limited by diffusion, then mass transfer coefficient or permeation rate is inversely proportional to membrane thickness. Similarly if mass transport is limited by interfacial mass transport, permeation rate becomes independent of membrane thickness.

## 4. RESULTS AND DISCUSSION

### 4.1. Fourier Transform Infrared Spectroscopy (FTIR)

Structure of the SPEEK sample was measured by FTIR spectroscopy method. FTIR of the SPEEK sample was measured on a Nicolet spectrometer (Magna IR-560) with the wavelength range of 450-4000  $\text{cm}^{-1}$ . Before testing, SPEEK sample was dried at 60°C for 5 minutes to ensure there was no moisture content. Figure 4 (a), (b), (c) represents the FTIR spectra of SPEEK sample with DS (0.38, 0.56 and 0.78) respectively. The C=O group present on the SPEEK sample was assigned on the wavelength range of 1600-1700  $\text{cm}^{-1}$ . That ensured the presence of ether group on the sample. The asymmetric O=S=O stretch was observed at 120-150  $\text{cm}^{-1}$  for DS (0.38) and 0.56. But it was at 1350  $\text{cm}^{-1}$  for DS (0.78). The symmetric O=S=O group was assigned at 1050  $\text{cm}^{-1}$ . The S=O group present on the sample was assigned on the range of 800-900  $\text{cm}^{-1}$ . There was a strong peak of O=S=O group

for DS (0.78) due the presence of more sulfonate group. Peak of the sulfonate group increased with increase in DS of the membrane. Very strong peak was observed for DS (0.78) membrane compared than other DS of membrane.

### 4.2. Water Uptake Results

Moisture uptake study was performed in a controlled humidity chamber. Steady state diffusion was observed at the initial stage of diffusion, so Fickian behavior is dominated. But when more water is absorbed, rate of diffusion decreases and relaxation rate governs diffusion process. In this case non Fickian behavior dominates. For better understanding of the Fickian and non-Fickian behavior, dual stage model was developed. Variation of moisture uptake data with exposure time was collected and fitted in a Fickian model proposed by Takamatsu et al. [28]. Experimental moisture uptake data with exposure time and its Fickian fit is shown in figure 5 (a). Experimental data is not appropriate fit on the Fickian model. At the initial stage of diffusion, Fickian model reasonably fits. But the later stage of diffusion, model could not correlate with experimental data due to relaxation rate dominant. But when the experimental data was fitted to a dual stage model, it gives appropriate fit. Appropriate fitting of experimental data in dual stage model is shown in figure 5(b). The Fickian and non-Fickian behavior of water diffusion can be well captured by dual stage model. Water diffusivity data of the different DS of membrane are calculated based on the dual stage model. Variation of water diffusivity with test temperature is shown in figure 6. It was observed that the diffusivity of water increased with membrane DS and temperature. As the test

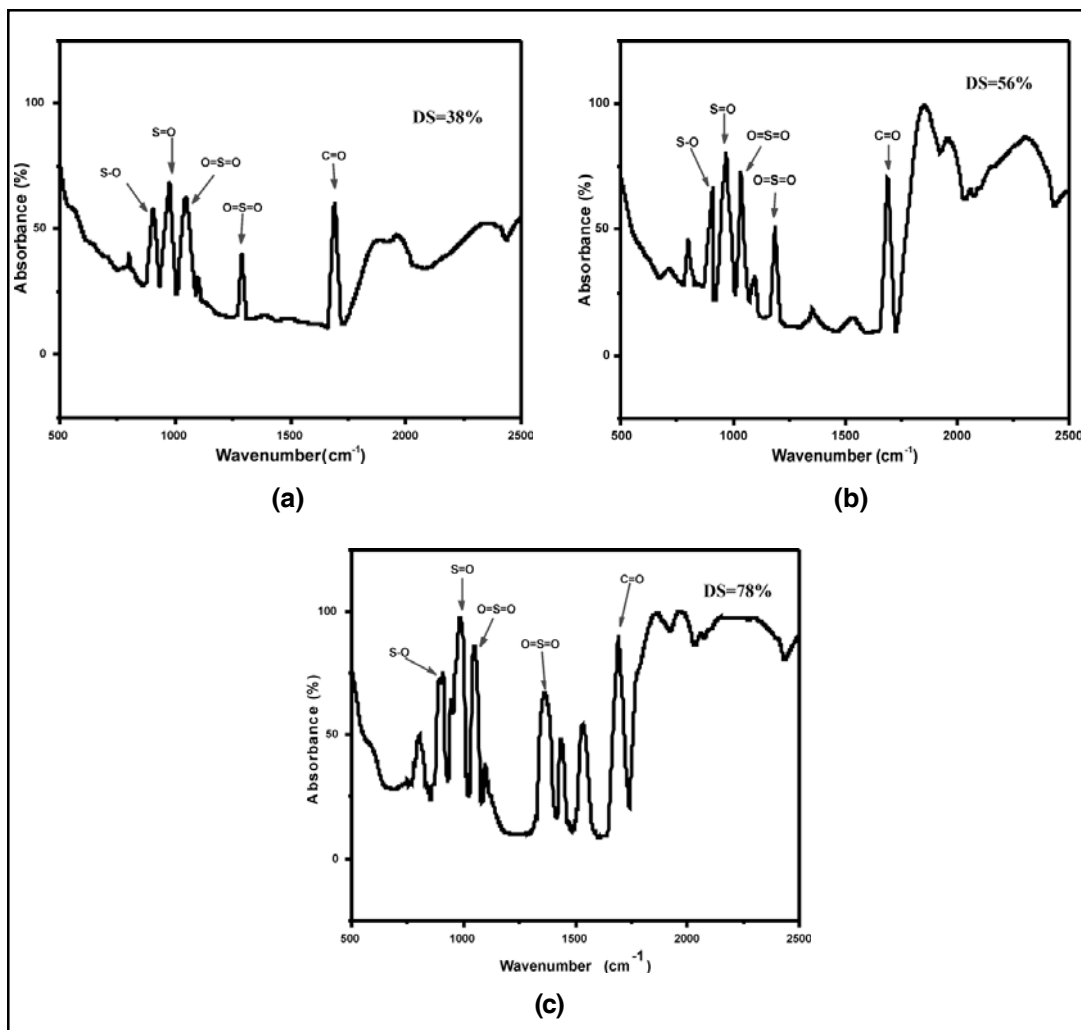


Fig. 4. (a) FTIR Spectra of SPEEK membrane with DS 38% (b) SPEEK membrane with DS 56% (c) SPEEK Membrane with DS 78%

temperature increased, kinetics of water molecule increases and boost diffusivity. At high temperature, membrane DS has the greatest effect on water diffusivity. At a fixed temperature, by improving DS from 0.38 to 0.56 diffusivity data increased more than 40% of its original value. Water diffusion study reveals that rate

of water diffusion increases with increase in temperature.

### 4.3. Liquid water permeation:

Liquid water was introduced on the fuel cell due to electrochemical reaction on fuel cell. Membrane water content plays important role

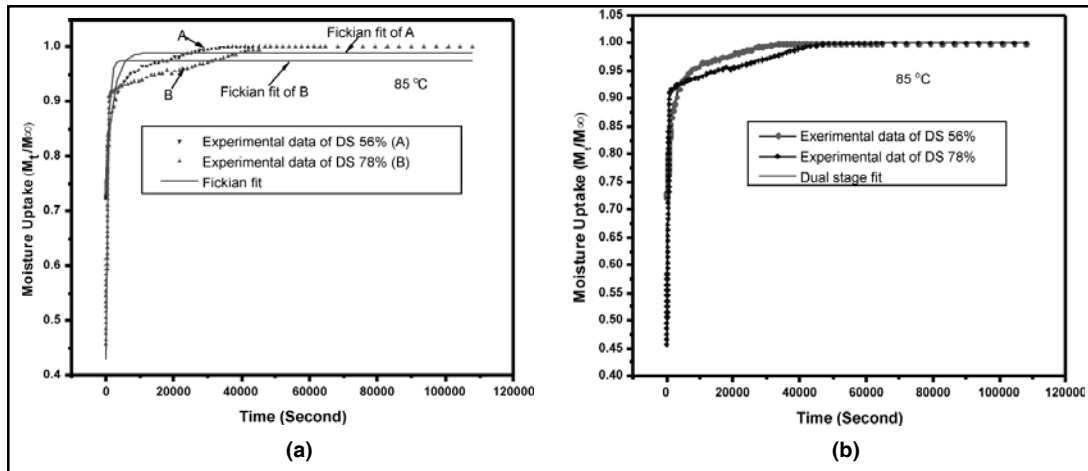


Fig. 5. Variation of moisture uptake with exposure time at 85°C for a membrane of DS (0.56, 0.78) with thickness of 127 $\mu$ . (a) Fickian fit of experimental moisture uptake data, (b) Dual stage fit of experimental moisture uptake data.

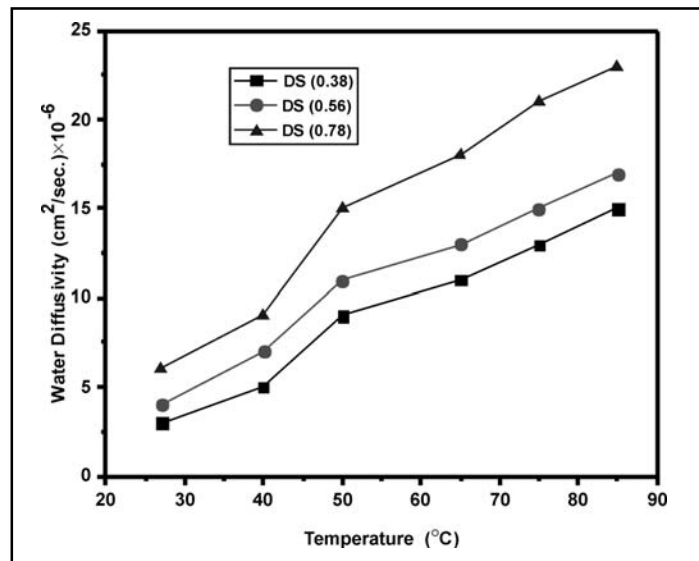


Fig. 6. Variation of water diffusivity with temperature for different DS of membrane

for fuel cell performance. For better performance, particular hydration level should be maintained on the membrane. Kinetics of water through membrane should be known

before practical application. Proton conductivity, which is very important parameter of fuel cell, depends on membrane water content. When water content exceed beyond hydration level,

fuel cell performance drastically decreased due to poor proton conductivity. Excess water can be discharged from the membrane to avoid poor performance. Kinetics of water depends on membrane thickness and DS. Water permeation study was performed by permeation cell at different temperature. For maintaining hydration of membrane, water should be uniformly distributed or transported across membrane area. So kinetic of water through membrane was vital for fuel cell performance. Water permeation rate across membrane was calculated from equation (8). Water permeation rate was performed at a temperature range of 40 and 85°C under proper controlled environment. Before performing permeation test, sample was immersed in distilled water to make proper hydration. Membrane with high DS (0.78) was considered for permeation test because of its high proton conductivity. From water permeation data, it was found that the rate of water permeation increases with increase in  $N_2$  flow rate on sweep side. As the sweep side Nitrogen flow rate increases, water activity decreases on the dry side of cell. In this case, water permeation rate approaches maximum.

Rate of water transport with sweep side Nitrogen flow rate at 40°C is shown in figure-7 (a). From permeation result, it shows that permeation rate was more for high DS membrane. This was due to the presence of more sulfonate group that retained more water molecule to improve hydrophilic domain suitable for water transport. Water permeation rate increased with increase in  $N_2$  flow rate on sweep side. Permeation results shows that the

rate of water transport was independent on membrane thickness at low Nitrogen flow rate. Majsztik et al. [31] suggested that when membrane was contacted with liquid water, rate of water transport was independent of thickness. Rate of water transport was dominated by diffusion and limited interfacial mass transport. At low Nitrogen flow rate, permeations result has good agreements with the theoretically proposed. But when Nitrogen flow rate exceeds 0.5 L/min., rate of water transport becomes dependent of membrane thickness. In this case, theory suggested by Majsztik et al. violates. Water transport across the membrane was controlled by both diffusion and interfacial mass transport. Permeation result shows that rate of water permeation varies inversely proportional with membrane thickness. For a particular membrane thickness, rate of water transport increases with increase in temperature and dry Nitrogen flow rate. At high temperature, interfacial mass transport increases between membrane/vapor interfaces. With increase in the interfacial mass transport, water permeation rate increases. Again at high temperature membrane swells more and creates more flow channel. Rate of water transport across membrane affect fuel cell performance. For improving fuel cell performance continuous removal of water was necessity. Water permeation result shows positive attribute towards fuel cell performance at high temperature. This was due to the excellent kinetic of water that boost discharge rate of excess water and enhance proton transport.

Water permeability data for different DS of membrane with thickness (127 $\mu$ m) was shown in figure 8.

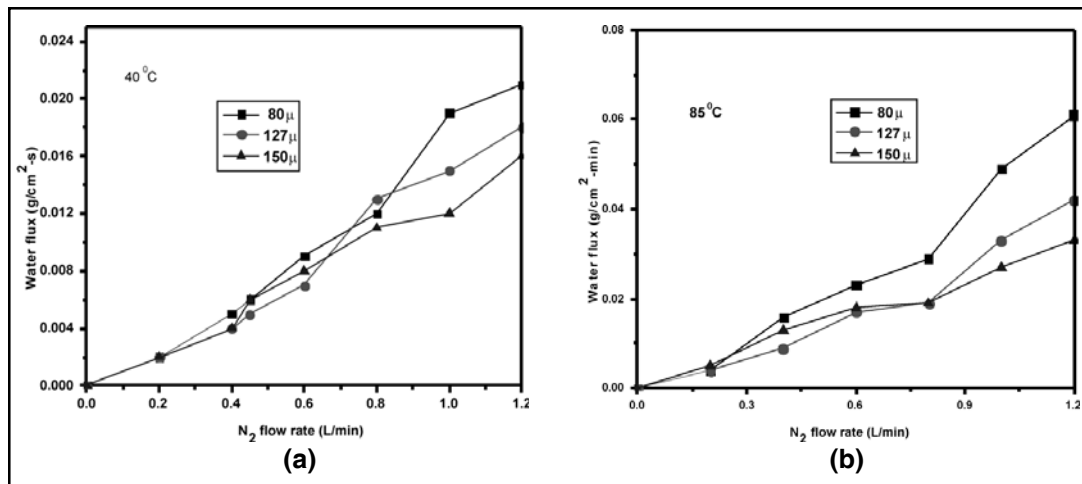


Fig. 7. Comparison of water permeation for different membrane thickness at (a) 40°C, (b) 85°C

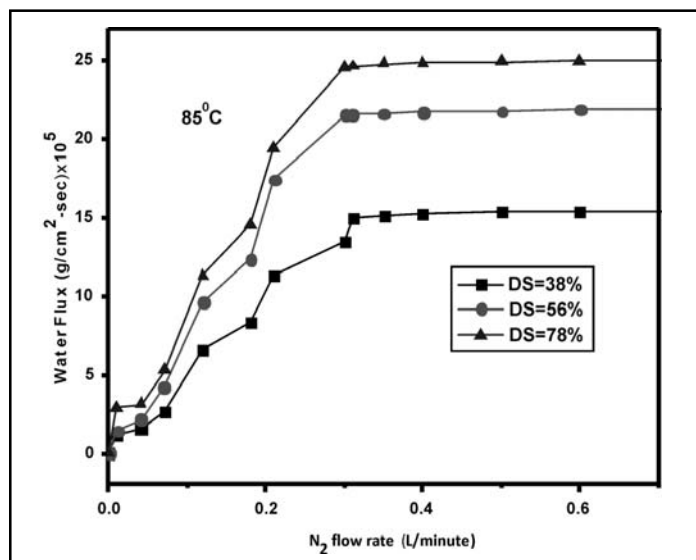


Fig. 8. Variation of water permeability with dry  $\text{N}_2$  flow rate for different membrane DS at 85°C

#### 4.4. Water vapor permeation

Humidified vapor was introduced on the feed side of permeation cell. It passed through the membrane due to the activity difference between feed and permeate side. Humidified

vapor was produced on the fuel cell due to high temperature operating condition. For maintaining desired hydration, role of water transport from humidified vapor was important. During water permeation study, water activity

at the feed side was maintained above 80% for steady state results. Permeation study was performed at a temperature range of 40-85°C with feed side water activity 80%. Permeation rate of water from humidified feed was shown in figure 9. During permeation studies, it was observed that SPEEK membrane shows better

stability to withstand at high temperature (85°C). Permeation results show that the rate of water permeation increased with increase in membrane temperature. It shows linear trend with sweep side N<sub>2</sub> flow rate and inversely proportional with membrane thickness.

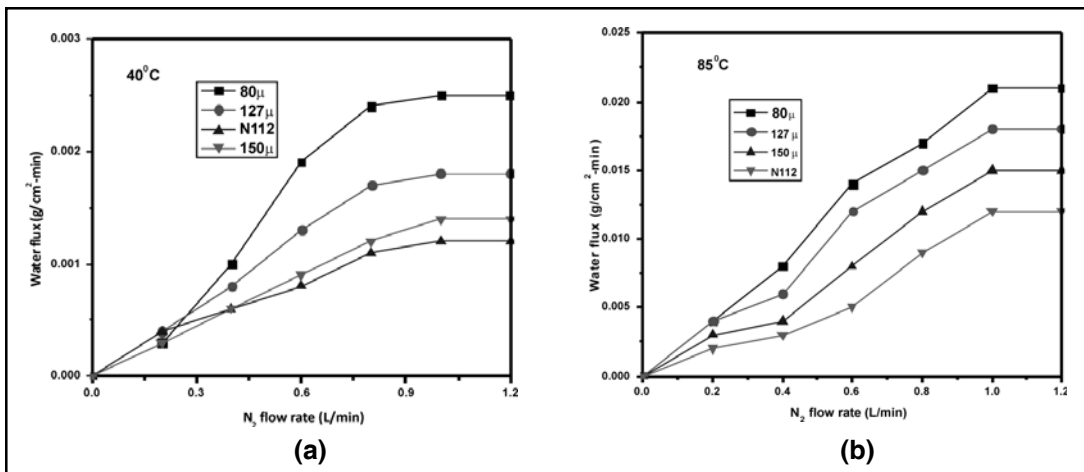


Fig. 9. Comparisons of water permeability from humidified feed (water activity 80%) at (a) 40°C (b) 85°C

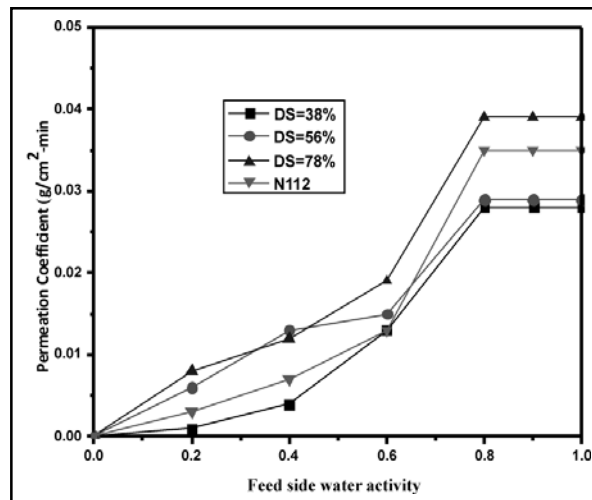


Fig. 10. Comparison of water permeability from humidified feed at different water activity for different membrane DS with thickness 127 μm at 85°C

Overall permeation coefficient of water through membrane was measured on permeation cell by considering interfacial mass transport and diffusion. Permeation coefficient (permeability) data was calculated by using equation (12). Variation of permeation coefficient with feed side water activity for different DS of membrane was shown in figure-10. Permeation results show that the permeability of water increases with increase in feed side water activity.

At low water activity, membrane with intermediate DS results better permeability of water. But when water activity exceeds 80%, membrane with high DS gave dominant permeability. It was found that SPEEK membrane with DS 78% shows better water permeability than Nafion membrane (N112) studied by Majsztrik et al.<sup>[31]</sup>. Because of its higher permeability, it can give better performance. It was concluded that at a fixed thickness and water activity SPEEK membrane give better proton conductivity than Nafion due to the volume fraction enhancement of hydrophilic domain.

## 5. CONCLUSION

IEC and DS of SPEEK membranes were increased with increase in reaction time. Proton conductivity data suggest that with increase in membranes DS; proton conductivity improved. Proton conductivity shows linear trend with membrane water content up to a particular extent then decreases. FTIR results confirmed the improvement of sulfonate group with increase in reaction time during synthesis process. Membrane with high DS provide better water uptake due to the presence of more sulfonate group. Volume fraction of hydrophilic domain increased with DS and ensured better

proton conductivity. Diffusivity of water increased with increase in DS and temperature of the membrane. Dual stage model predict appropriate fit of experimental water uptake data. Study reveals that at the initial stage of diffusion, moisture uptake follows Fickian diffusion. But later stage of diffusion, non Fickian behavior (relaxation rate dominate) was observed. Fuel cell can accord better performance at high temperature, due to the excellent removal of excess water and better water transport across the membrane. Liquid water transport was inversely proportional with membrane thickness and was controlled by both diffusion and interfacial mass transport. From vapor feed, rate of water permeation increased with increase in membrane temperature. SPEEK membrane accords better water permeation rate than Nafion at a specified condition. Water permeation rate provide linear trend with sweep side N<sub>2</sub> flow rate due to more water activity gradient. Rate of water transport was more for liquid water than humidified vapor feed. Permeation results show that the permeability of water increases with increase in feed side water activity. At low water activity, membranes with intermediate DS perform better permeability. But when water activity exceeds 80%, membranes with high DS perform better permeation rate. Permeation and diffusion result suggest that membrane with high DS provide better performance at high temperature due to its ability of high water diffusion and permeation rate.

## REFERENCES

1. An introduction to the 2010 fuel cell pre-solicitation workshop, Department of Energy, Lakewood, Colorado; 2010.

2. Majsztzik, P. W.; Satterfield, M. B.; Bocarsly, A. B.; Benziger, J. B. *Journal of Membrane Science*, 2007, 301, 93.
3. Zawodzinski, T. A.; Derouin, C.; Radzinski, S.; Sherman, R. J.; Smith, V. T.; Springer, T. E.; Gottesfeld S., *Journal of Electrochemical Society*, 1993,140, 1041.
4. Rivin, D.; Kendrick, C. E.; Gibson, P. W.; Schneider, N. S., *Polymer*, 2001, 42, 623.
5. Takamatsu, T.;Hashiyama, M.; Eisenberg, A., *Journal of Applied Polymer Science*, 1979, 24, 2199.
6. Morris, D. R.; Sun, X. D. *Journal Applied Polymer Science*, 1993, 50, 1445.
7. Krtil, P.; Trojanek, A.; Samec, Z., *Journal of Physical Chemistry B*, 2001, 105, 7979.
8. Burnett, D. J.; Garcia, A. R.; Thielmann, F., *Journal of Power Sources*, 2006, 160, 426.
9. Rhim, J. W.; Park, H. B.; Lee, C. S.; Jun, J. H.; Kim, D. S.; Lee, Y. M., *Journal of Membrane Science*, 2004, 238, 143.
10. Xu, W.; Liu, C.; Xue, X.; Su, Y.; Ln, Y.; Xing, W.; Lu, T., *Solid State Ionics*, 2004, 171, 121.
11. Tsai, C. E.; Lin, C. W.; Hwang, B. J., *Journal of Power Sources*, 2010, 195, 2166.
12. Shao, Z. G.; Wang, X.; Hsing, I. M., *Journal of Membrane Science*, 2002, 210, 147.
13. Kang, M. S.; Kim, J. H.; Won, J. W.; Moon, S. H.; Kang, Y. S., *Journal of Membrane Science*, 2005, 247, 127.
14. Kim, D. S.; Park, H. B.; Rhim, J. W.; Lee, Y. M., *Solid State Ionics*, 2005, 176, 117.
15. Xing, P. X.; Robertson, G. P.; Guiver, M. D.; Mikhailenko, S. D.; Wang, K. P.; Kaliaguine, S., *Journal of Membrane Science*, 2004, 229, 95.
16. Jaafar, J.; Ismail, A. F.; Mustafa, A. *Material Science and Engineering: A*, 2007,460, 475.
17. Zaidi, S. M. J.; Mikhailenko, S. D.; Robertson, G. P.; Guiver, M. D.; Kaliaguine, S., *Proton conducting Journal of Membrane Science*, 2000, 173, 17.
18. Bauer, B.; Jones, D. J.; Roziere, J.; Tchicaya, L.; Alberti, G.; Casciola, M.; Massinelli, L.; Peraio, A.; Besse, S.; Ramunni, E., *Journal of New Materials for Electrochemical System*, 2000, 3, 93.
19. Luu, D. X.; Cho, E. B.; Han, O. H.; Kim, D., *Journal of Physical Chemistry B*, 2009, 113, 30.
20. Ge, S. H.; Li, X. G.; Yi, B. L.; Hsing, I. M. *Journal of Electrochemical Society*, 2005, 152, A1149-A1157.
21. Thampan, T.; Malhotra, S.; Tang, H.; Datta, R., *Journal of Electrochemical Society*, 2000, 147, 3242–3250.
22. Weber, A. Z.; Newman, J. *American Institute of Chemical Engineers Journal*, 2004, 50, 3215–3226.
23. Zawodzinski, T. A.; Derouin, C.; Radzinski, S.; Sherman, R. J.; Smith, V. T.; Springer, T. E.; Gottesfeld, S.; *Journal of Electrochemical Society*, 1993, 140, 1041–1047.
24. Doyle, M.; Rajendran, G. *Fuel Cell Technology and Applications*; Vielstich, W., Gasteiger, H. A., Lamm, A., Eds.; Wiley: New York, 2003; Vol. 3.
25. Satterfield, M. B., *Mechanical and Water Sorption Properties of Nafion and Composite Nafion/Titanium Dioxide Membranes for Polymer Electrolyte Membrane Fuel Cells. Ph.D. Thesis*, Princeton University, 2007.
26. Yeo, S. C.; Eisenberg, A. *Journal of Applied Polymer Sci.* 1977, 21, 875–898.
27. Kim KH, Lee KY, Lee SY, Cho EA, Lim TH, Kim HJ, et al. *International Journal of Hydrogen Energy*, 2010, 35, 13104-10.
28. T. Takamatsu, M. Hashiyama, A. Eisenberg, *J. Appl. Polym. Sci.* 24 (11) (1979) 2199–2220.
29. D.R. Morris, X.D. *J. Appl. Polym. Sci.* 50 (8) (1993) 1445–1452.
30. Mark D. Placette, Xuejun Fan, Jie Hua Zhao and Darvin Edwards, *A dual stage model of anomalous moisture diffusion and desorption*

*in epoxy mold compounds*, 12<sup>th</sup> international conference on thermal, mechanical and multiphysics, simulation and experiments in microelectronics and Microsystems, EuroSimE, 2011.

31. Paul Majsztzik, Andrew Bocarsly, and Jay Benziger, *Journal of Physical Chemistry B*, 2008, 112, 16280–16289.

Received: 08-03-2018

Accepted: 16-03-2018